Available online at www.sciencedirect.com
ScienceDirect
Mathematics and Computers in Simulation 74 (2007) 82–92
MATHEMATICS AND COMPUTERS IN SIMULATION
www.elsevier.com/locate/matcom

Fourier–Galerkin method for 2D solitons of Boussinesq equation

M.A. Christou[a], C.I. Christov[b,*]

[a] *Department of Mathematics, University of Cyprus, Cyprus*
[b] *Department of Mathematics, University of Louisiana at Lafayette, LA, USA*

Available online 28 November 2006

Abstract

We develop a Fourier–Galerkin spectral technique for computing the stationary solutions of 2D generalized wave equations. To this end a special complete orthonormal system of functions in $L^2(-\infty, \infty)$ is used for which product formula is available. The exponential rate of convergence is shown. As a featuring example we consider the Proper Boussinesq Equation (PBE) in 2D and obtain the shapes of the stationary propagating localized waves. The technique is thoroughly validated and compared to other numerical results when possible.

PACS: 02.60.Cb; 02.70.Hm

Keywords: Galerkin spectral method; Boussinesq equation; Solitons

1. Introduction

One of the most important features of generalized wave equations containing nonlinearity and dispersion, is that they possess solutions of type of permanent waves which behave in many instances as particles. When the governing system is fully integrable, such waves are called *solitons*. In 1D a plethora of deep mathematical results have been obtained for solitons [7,18,1]. The success was contingent upon the existence of an analytical solution of the respective nonlinear dispersive equation. Naturally, predominant part of the theoretical results were confined to the 1D case. It is of high importance to investigate the 2D case, which in most of the cases, can be done only numerically.

The first soliton-supporting generalized wave equation (GWE) was derived by Boussinesq [2] who found its permanent solution to be of *sech* type. The existence of a localized solution proved that a balance between dispersion and nonlinearity exist. Later on Korteweg and de Vries [17] derived the evolution equation for the wave amplitude in the moving frame. The same *sech* is a solution also to KdV equation. To the family of soliton-supporting models that attracted enormous attention in the recent years, one can also add Sine-Gordon and Schrödinger equations. For all these equations, finding 2D solitary wave is a must. One should be able to apply the algorithm developed here for the Boussinesq equation to other soliton-supporting equations.

Targeting a localized solution imposes special requirements on the numerical technique to be used because no boundary conditions are specified at given points, but rather the square of solution is required to be integrable over the infinite domain. Such solution is said to belong to the $L^2(-\infty, \infty)$ space. A number of difficulties are encountered on the way of application of difference or/and finite-element numerical methods to the problems in $L^2(-\infty, \infty)$. One of

* Corresponding author. Tel.: +1 337 482 5273; fax: +1 337 482 5346.
E-mail address: christov@louisiana.edu (C.I. Christov).

0378-4754/$32.00 © 2006 IMACS. Published by Elsevier B.V. All rights reserved.
doi:10.1016/j.matcom.2006.10.002

the worst setbacks lies in the inevitable reducing of the infinite interval to a finite one. Such a procedure introduces artificial eigenvalue problems This difficulty can be surmounted if a spectral method is used with basis system of localized functions which automatically acknowledge the requirement that the solution belongs to $L^2(-\infty, \infty)$ space. Here we make use of a complete orthonormal (CON) system of functions proposed in [13]. In a sequence of papers Boyd [4,5] showed a general way of constructing CON systems in $L^2(-\infty, \infty)$ by means of coordinate transformation to a finite interval and consecutive use of Chebyshev polynomials (see [6] for complete reference). The rational functions [13] are orthogonal without weight and possess an expression for the product of two members of the system into series with respect to the system (as do the Chebyshev–Boyd functions, but the latter are orthogonal with weight). The product property is crucial because it allows one to use a Galerkin type of expansion the latter being much simpler and faster in implementation than the pseudo-spectral algorithm.

A Fourier–Galerkin technique based on the CON system [13] was applied first to KdV and Kuramoto-Sivashinsky equation in [15]. In [10], the performance of the chosen system was demonstrated and has been extended to equations with cubic nonlinearity. The case of solitons with oscillatory tails was treated in [9]. The time dependent problem of interacting 1D solitons was solved in [11,12], but the situation there is different because a superposition of analytical *sech* solutions is available to be used as initial condition. In 2D, the first problem to solve is to find the individual shape of the solitary wave. To this problem is devoted the present paper. The application the CON system [13] to 2D was initiated in [14] but for the simpler model problem of quadratic Klein–Gordon equation (KGE). KGE is of second order with respect to spatial derivatives while here we deal with a fourth-order GWE which requires further development of the technique.

2. Boussinesq model of surface waves

We consider the 2D Proper Boussinesq Equation (PBE)

$$u_{tt} = \Delta[u - u^2 - \Delta u]$$

where $\beta > 0$ is the dispersion parameter, α the amplitude parameter, and γ is the characteristic speed of the small disturbances. In our case the solitary wave solution is subject to the asymptotic boundary conditions (a.b.c) $u(t, x, y) \to 0$, for $x, y \to \pm\infty$.

Upon introducing an auxiliary function q one can show that the PBE follows from the system

$$u_{tt} = \Delta q, \qquad q = u - u^2 - \delta\Delta u, \tag{1}$$

with boundary conditions

$$u \to 0, q \to 0, \quad \text{for}\, x \to \pm\infty,\ y \to \pm\infty. \tag{2}$$

Let us consider the case of stationary propagating wave and c_1 and c_2 are the components of the phase speed of the center of the localized structure. In a frame moving with the wave one can introduce new independent variables

$$\tilde{x} = x - c_1 t \quad \text{and} \quad \tilde{y} = y - c_2 t.$$

Upon introducing ξ and η into Eq. (1) we get an elliptic system for the stationary localized solution. Since re-scaling the spatial variables ξ and η does not change the nature of the asymptotic boundary value problem considered here, we introduce the scalings $\tilde{x} = \lambda\xi$, $\tilde{y} = \mu\eta$ and arrive at the following system for the shape of stationary propagating wave of Boussinesq equation:

$$\begin{aligned} 0 &= \lambda^{-2} q_{\xi\xi} + \mu^{-2} q_{\eta\eta} - [\lambda^{-2} c_1^2 u_{\xi\xi} + 2\lambda^{1}\mu^{-1} c_1 c_2 u_{\xi\eta} + \mu^{-2} c_2^2 u_{\eta\eta}], \\ 0 &= q - u + u^2 + \lambda^{-2} u_{\xi\xi} + \mu^{-2} u_{\eta\eta}. \end{aligned} \tag{3}$$

Using the scaling parameters is crucial because they allow one to adjust the characteristic length of the CON system of functions, to the characteristic length of the sought solution. The importance of the scaling parameter was elucidated in the comprehensive monograph on spectrum methods [6] where it was shown how the scaling can be included in the definition of the rational functions from the basis. For series based on Hermit polynomials, the scaling is discussed in [3]. In the previous works of the authors [9–11], the role of the scaling in 1D problems is demonstrated quantitatively. In the present paper, we will use the optimal values of the scaling parameters without going into details how they were selected.

3. Iterative procedure: operator-splitting scheme

We introduce artificial time in system Eq. (3) and use a time stepping scheme as an iterative procedure to obtain the solution of the elliptic system. In order to achieve second order of approximation in time we use staggered time stages for the two functions. To make the time stepping computationally efficient we use the method of operator splitting [20], arriving at the following scheme:

$$\begin{aligned}
\frac{\tilde{q}-q^{n-(1/2)}}{\tau} &= \lambda^{-2}\tilde{q}_{\xi\xi}+\mu^{-2}q^{n-(1/2)}_{\eta\eta}-[\lambda^{-2}c_1^2u^n_{\xi\xi}+2\lambda^{-1}\mu^{-1}c_1c_2u^n_{\xi\eta}+\mu^{-2}c_2^2u^n_{\eta\eta}]\\
\frac{q^{n+(1/2)}-\tilde{q}}{\tau} &= \mu^{-2}q^{n+(1/2)}_{\eta\eta}-\mu^{-2}q^{n-(1/2)}_{\eta\eta}\\
\frac{\tilde{u}-u^n}{\tau} &= \lambda^{-2}\tilde{u}_{\xi\xi}+\mu^{-2}u^n_{\eta\eta}+q^{n+(1/2)}-u^n+(u^n)^2\\
\frac{u^{n+1}-\tilde{u}}{\tau} &= \mu^{-2}u^{n+1}_{\eta\eta}-\mu^{-2}u^n_{\eta\eta}
\end{aligned} \tag{4}$$

The intermediate functions $\tilde{q}$, $\tilde{u}$ can be eliminated to get “the full-time-step scheme”.

$$\begin{aligned}
&(I+\mu^{-2}\lambda^{-2}\tau^2\partial_{\xi\xi}\partial_{\eta\eta})\frac{q^{n+(1/2)}-q^{n-(1/2)}}{\tau} = (\mu^{-2}\partial^2_{\eta\eta}+\lambda^{-2}\partial_{\xi\xi})q^{n+(1/2)}\\
&\quad-(\lambda^{-2}c_1^2u^n_{\xi\xi}+2\lambda^{-1}\mu^{-1}c_1c_2u^n_{\xi\eta}+\mu^{-2}c_2^2u^n_{\eta\eta})\\
&(I+\mu^{-2}\lambda^{-2}\tau^2\partial_{\xi\xi}\partial_{\eta\eta})\frac{u^{n+1}-u^{n-1}}{\tau} = (\mu^{-2}\partial^2_{\eta\eta}+\lambda^{-2}\partial_{\xi\xi})u^{n+1}+q^{n+(1/2)}-u^n+(u^n)^2,
\end{aligned}$$

where I is the identity operator. The mixed second derivatives and the nonlinear term are approximated explicitly and as a result, the above scheme is not fully implicit. However, its margin of stability is wide enough and one can choose the increment τ in wide intervals only on the basis of considerations to optimize the rate of convergence. When the iterations converge for $n\to\infty$, we get that $q^{n+(1/2)}\to q^{n-(1/2)}$, $u^{n+1}\to u^n$ which means that the solution of the original elliptic system, Eq. (3), is obtained.

The method of artificial time is stable because the spatial operators in the right-hand sides of the equations are negative definite.

4. Fourier–Galerkin method in $L^2(-\infty,\infty)$

From the known spectral techniques we choose Galerkin method because it has the advantage of simplicity in implementation in comparison with the spectral collocation method or tau-method (see the arguments in [6]). The Galerkin technique requires explicit formulas expressing the products of members of the complete orthonormal (CON) system into series with respect to the system. We use the CON system introduced in [13]

$$S_n=\frac{\rho_n+\rho_{-n-1}}{\mathrm{i}\sqrt{2}},\qquad C_n=\frac{\rho_n-\rho_{-n-1}}{\sqrt{2}},\qquad \rho_n(x)=\frac{1}{\sqrt{\pi}}\frac{(\mathrm{i}x-1)^n}{(\mathrm{i}x+1)^{n+1}}, \tag{5}$$

where functions $\rho_n(x)$, $n=0,1,2,\ldots$ were derived by Wiener [19], as Fourier transforms of the Laguerre functions (functions of parabolic cylinder). Higgins [16] defined the functions with negative indexes n and proved the completeness and orthogonality of the system. The significance of the above system for nonlinear problems for localized solutions was demonstrated in [13], where the product formula was derived. Following the notations form [15] we have:

$$C_nC_k=\sum_{m=1}^{\infty}\beta_{nk,m}C_m,\qquad S_nS_k=\sum_{m=1}^{\infty}\alpha_{nk,m}C_m,\qquad S_nC_k=\sum_{m=1}^{\infty}\gamma_{nk,m}S_m, \tag{6}$$

$$\alpha_{nk,m} = \frac{1}{2\sqrt{2\pi}}\left\{\delta_{m,n+k+1} + \delta_{m,|n-k|} - \delta_{m,n+k} - \operatorname{sgn}\left[|n-k| - \frac{1}{2}\right]\delta_{m,[|n-k|-(1/2)]}\right\},$$

$$\beta_{nk,m} = \frac{1}{2\sqrt{2\pi}}\left\{\delta_{m,n+k} + \delta_{m,|n-k|} - \delta_{m,n+k+1} - \operatorname{sgn}\left[|n-k| - \frac{1}{2}\right]\delta_{m,[|n-k|-(1/2)]}\right\},$$

$$\gamma_{nk,m} = \frac{1}{2\sqrt{2\pi}}\{\delta_{m,n+k} + \operatorname{sgn}(n-k)\delta_{m,|n-k|} - \delta_{m,n+k+1} - \operatorname{sgn}(n-k)\delta_{m,|n-k|-1}\},$$

which allows one to develop a Galerkin technique based on this system of functions.

For the first and second derivative of the basis functions one has (see [13])

$$C_n' = -\sum_{m=0}^{\infty}\theta_{m,n}S_m, \qquad S_n' = -\sum_{m=0}^{\infty}\theta_{m,n}C_m,$$

$$\theta_{m,n} = \tfrac{1}{2}n\delta_{m,n-1} - \tfrac{1}{2}(2n+1)\delta_{m,n} + \tfrac{1}{2}(n+1)\delta_{m,n+1},$$

$$C_n'' = \sum_{m=0}^{\infty}\chi_{m,n}C_m, \qquad S_n'' = \sum_{m=0}^{\infty}\chi_{m,n}S_m,$$

$$\chi_{m,n} = -\tfrac{1}{4}n(n-1)\delta_{m,n-2} + n^2\delta_{m,n-1} - \tfrac{1}{4}(n+1)(n+2)\delta_{m,n+2} - \tfrac{1}{4}n^2 + (2n+1)^2 + (n+1)^2\delta_{m,n} + (n+1)^2\delta_{m,n+1}.$$

Matrix χ is penta-diagonal, which allows using efficient algorithms for banded matrices.

The most important issue for a spectral method is its rate of convergence which can be shown through the following relationship between the Fourier periodic functions and our system, namely:

$$C_n(x) = (-1)^n\frac{\cos(n+1)\theta + \cos n\theta}{\sqrt{2}}, \qquad S_n(x) = (-1)^{n+1}\frac{\sin(n+1)\theta + \sin n\theta}{\sqrt{2}},$$

where $x = \tan(\theta/2)$ or $\theta = 2\arctan(x)$ is a transformation of the independent variable. Note that any function $f(x)$ is a periodic function of θ with period 2π. Since, the Fourier series have exponential convergence for periodic functions, then the exponential convergence of C_n, S_n series follows (see, [12]).

We develop the sought functions u, q into series with respect to the subsequences C_n and S_n namely,

$$u(\xi,\eta) = \sum_{m=0}^{\infty}\sum_{n=0}^{\infty}[a_{mn}C_m(\xi)C_n(\eta) + b_{mn}S_m(\xi)S_n(\eta)],$$
$$q(\xi,\eta) = \sum_{k=0}^{\infty}\sum_{j=0}^{\infty}[d_{kj}C_k(\xi)C_j(\eta) + e_{kj}S_k(\xi)S_j(\eta)], \tag{7}$$

and the superscripts and/or tildes of the functions carry on to the coefficients when necessary.

Introducing Eq. (7) into Eq. (4) and making use the orthogonality of the system of basis functions we arrive, for the even functions, to the following coupled systems for the first half-time step:

$$\frac{\tilde{d}_{mn} - d_{mn}^{l-(1/2)}}{\tau} = \lambda^{-2}\sum_{k=0}^{\infty}\sum_{j=0}^{\infty}\tilde{a}_{kj}\chi_{kj} + \mu^{-2}\sum_{k=0}^{\infty}\sum_{j=0}^{\infty}d_{kj}^{l-(1/2)}\chi_{kj} - \lambda^{-2}c_1^2\sum_{k=0}^{\infty}\sum_{j=0}^{\infty}a_{kj}^l\chi_{kj} - 2\lambda^{-1}\mu^{-1}c_1c_2 \times\sum_{k=0}^{\infty}\sum_{j=0}^{\infty}a_{kj}^l\theta_{kj}\theta_{kj} - \mu^{-2}c_2^2\sum_{k=0}^{\infty}\sum_{j=0}^{\infty}a_{kj}^l\chi_{kj}$$

$$\frac{\tilde{a}_{mn} - a_{mn}^l}{\tau} = \lambda^{-2}\sum_{k=0}^{\infty}\sum_{j=0}^{\infty}d_{kj}^{l+(1/2)}\chi_{kj} + \mu^{-2}\sum_{k=0}^{\infty}\sum_{j=0}^{\infty}a_{kj}^l\chi_{kj} + d_{mn}^{l+(1/2)} - a_{mn}^l + \Phi_{ij},$$

where Φ_{ij} is the coefficient of the expansion of the nonlinear term into series into the system. For the specific CON system it reads,

$$\sum_{k_1=0}^{\infty}\sum_{k_2=0}^{\infty}\sum_{m_1=0}^{\infty}\sum_{m_2=0}^{\infty}[a^l_{k_1m_1}a^l_{k_2m_2}\beta_{k_1k_2m_1m_2,mn}+b^l_{k_1m_1}b^l_{k_2m_2}\alpha_{k_1k_2m_1m_2,mn}],$$

but it is inefficient to use above expression and face the evaluation of fourtuple sums. Instead, as shown in [12] we can use the "convolution" sums. We illustrate here the idea of these sums for one of the variable, making use of the explicit expression for β_{mnl}, namely

$$\sum_{n=0}^{N}\sum_{m=0}^{N}u_nu_mC_nC_m=\sum_{l=0}^{N}\left[\sum_{n=0}^{N}\sum_{m=0}^{N}\beta_{nml}u_nu_m\right]C_l\stackrel{\text{def}}{=}\frac{1}{2\sqrt{2\pi}}\sum_{l=0}^{N}b_lC_l,$$
$$b_l=\sum_{n=0}^{l-1}u_nu_{l-1-n}-\sum_{n=0}^{l}u_nu_{l-n}-2\sum_{n=l}^{N}u_nu_{n-l}+2\sum_{n=l+1}^{N}u_nu_{n-l-1}, \tag{8}$$

where u_i are the coefficients. Applying Eq. (8) twice for each of the variables x and y we reduce the fourtuple sum for the coefficients to double sum, which gives a radical reduction of the number of calculations per node.

The second half-time step is the "stabilizing correction" given by the following:

$$\frac{a^{l+1}_{mn}-\tilde a_{mn}}{\tau}=\mu^{-2}\sum_{k=0}^{\infty}\sum_{j=0}^{\infty}a^{l+1}_{kj}\chi_{kj}-\mu^{-2}\sum_{k=0}^{\infty}\sum_{j=0}^{\infty}a^{l}_{kj}\chi_{kj},$$

$$\frac{d^{l+(1/2)}_{mn}-\tilde d_{mn}}{\tau}=\mu^{-2}\sum_{k=0}^{\infty}\sum_{j=0}^{\infty}d^{l+(1/2)}_{kj}\chi_{kj}-\mu^{-2}\sum_{k=0}^{\infty}\sum_{j=0}^{\infty}d^{l-(1/2)}_{kj}\chi_{kj}.$$

In a similar fashion is obtained the systems for the coefficients of odd functions

$$\frac{\tilde e_{mn}-e^{l-(1/2)}_{mn}}{\tau}=\lambda^{-2}\sum_{k=0}^{\infty}\sum_{j=0}^{\infty}\tilde e_{kj}\chi_{kj}+\mu^{-2}\sum_{k=0}^{\infty}\sum_{j=0}^{\infty}e^{l-(1/2)}_{kj}\chi_{kj}-\lambda^{-2}c_1^2\sum_{k=0}^{\infty}\sum_{j=0}^{\infty}b^l_{kj}\chi_{kj}$$
$$-2\lambda^{-1}\mu^{-1}c_1c_2\sum_{k=0}^{\infty}\sum_{j=0}^{\infty}b^l_{kj}\theta_{kj}\theta_{kj}-\mu^{-2}c_2^2\sum_{k=0}^{\infty}\sum_{j=0}^{\infty}b^l_{kj}\chi_{kj}$$

$$\frac{\tilde b_{mn}-b^l_{mn}}{\tau}=\lambda^{-2}\sum_{k=0}^{\infty}\sum_{j=0}^{\infty}e^{l+(1/2)}_{kj}\chi_{kj}+\mu^{-2}\sum_{k=0}^{\infty}\sum_{j=0}^{\infty}b^l_{kj}\chi_{kj}+e^{l+(1/2)}_{mn}-b^l_{mn}+\Psi_{mn},$$

where

$$\Psi_{mn}=2\sum_{k_1=0}^{\infty}\sum_{k_2=0}^{\infty}\sum_{m_1=0}^{\infty}\sum_{m_2=0}^{\infty}a^l_{k_1m_1}b^l_{k_2m_2}\gamma_{k_1k_2m_1m_2,mn},$$

is the nonlinear term for which a formula similar to Eq. (8) is derived to render the fourtuple sum to a double sum. Respectively, the second half-time step is given by

$$\frac{e^{l+(1/2)}_{mn}-\tilde e_{mn}}{\tau}=\mu^{-2}\sum_{k=0}^{\infty}\sum_{j=0}^{\infty}e^{l+(1/2)}_{kj}\chi_{kj}-\mu^{-2}\sum_{k=0}^{\infty}\sum_{j=0}^{\infty}e^{l-(1/2)}_{kj}\chi_{kj}$$

$$\frac{b^{l+1}_{mn}-\tilde b_{mn}}{\tau}=\mu^{-2}\sum_{k=0}^{\infty}\sum_{j=0}^{\infty}b^{l+1}_{kj}\chi_{kj}-\mu^{-2}\sum_{k=0}^{\infty}\sum_{j=0}^{\infty}b^{l}_{kj}\chi_{kj}$$

In order to avoid the trivial solution we consider the re-scaled vector $a=\alpha\hat a$ (where α is unknown parameter) and impose a condition on the first coefficient, say $\hat a_{00}=-1$, which makes the system for the coefficients overposed. In order to avoid this problem the equation for $\hat{a_{00}}$ should not be used together with the rest of the algebraic equations when solving for $\hat{a}_{ij}$. Rather, it becomes an explicit relation for determination of α. After a^{l+1} is obtained, the current iteration for α^{l+1} is given by

$$\alpha^{n+1} = \frac{\tilde{p}_{00}}{\tau\mu^{-2}(\sum_{k=0}^{\infty}\sum_{j=0}^{\infty} a_{kj}^{l+1}\chi_{kj} - \sum_{k=0}^{\infty}\sum_{j=0}^{\infty} a_{kj}^{l}\chi_{kj})}.$$

The initial condition is taken $\alpha^0 = 1$ and then it is iteratively improved according to the above formula with the time stepping of the coefficients.

Here a note on the computational efficiency of the method is due. If the pseudo-spectral method is employed, one can use the Fast Fourier Transform. Being reminded that the FFT requires $O(5\log(N)N)$ operations, one can easily estimate that at $N = 20$ the pseudo-spectral method becomes more efficient than the Galerkin method (N^2 operations) for the same number of modes from the mere point of view of the number of multiplications per node. However, if the aim is to achieve the same accuracy, one has to use much larger number of nodes in the pseudo-spectral method than in the Galerkin method in order to reduce the discretization error. From this point of view we can place the threshold roughly at $N = 50$, but this number may increase further if highly oscillating solutions are encountered for which the discretization error is larger.

Speaking about difference methods, we actually did compare with a difference solution in Section 6 of this paper. We can only add here that the same accuracy reached by the Galerkin method with 20 nodes (20**3 = 800 operations) can be obtained only for $N = 1600$ points which makes $N^2 = 1600^2 = 2{,}560{,}000$ operations. Clearly, finite differences are not the method of choice for problems on infinite domains.

5. Tests and validations

To validate the performance of the method we begin with the case $c_1 = c_2 = 0$ when the solution possesses radial symmetry and depends only on $r = \sqrt{x^2 + y^2}$.

First, we check the asymptotic rate of convergence of our algorithm. For the case with radial symmetry, it suffice to consider the behavior of the series $P_i = |p_{ii}|$, where p_{ii} are the even Galerkin coefficients for sought function u. In the case of radial symmetry one can set the scales equal to each other. As already above mentioned, the theoretical rate of convergence of our series is exponential, hence the expected behavior is $P_i \sim e^{-qi}$. Fig. 1(a) shows the result obtained for different total number of functions N.

The exponential decay is clearly observed with a best fit function

$$P_i = p_{ii} = 0.0005\,e^{-0.085i}.$$

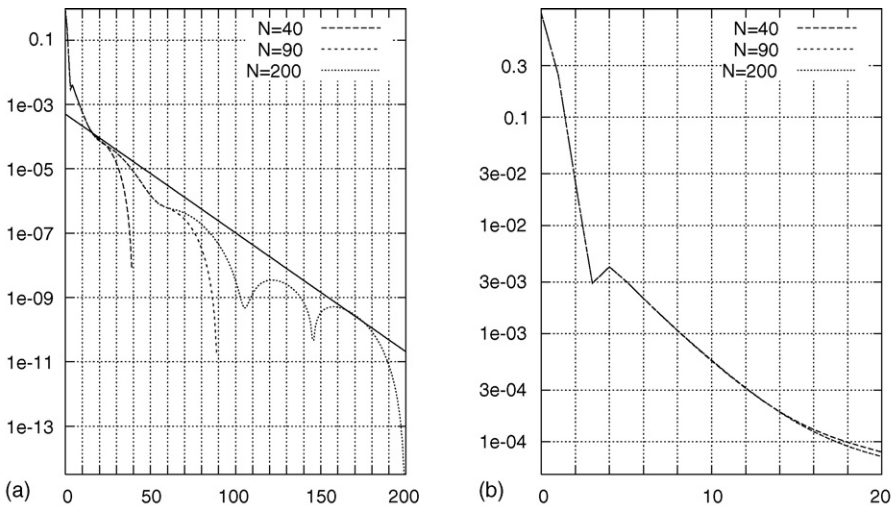

Fig. 1. The absolute value of a coefficient as function of its number for three different total numbers of functions N: (a) asymptotic decay of coefficients—$0.0005\,e^{-0.085x}$ and (b) first 21 coefficients.

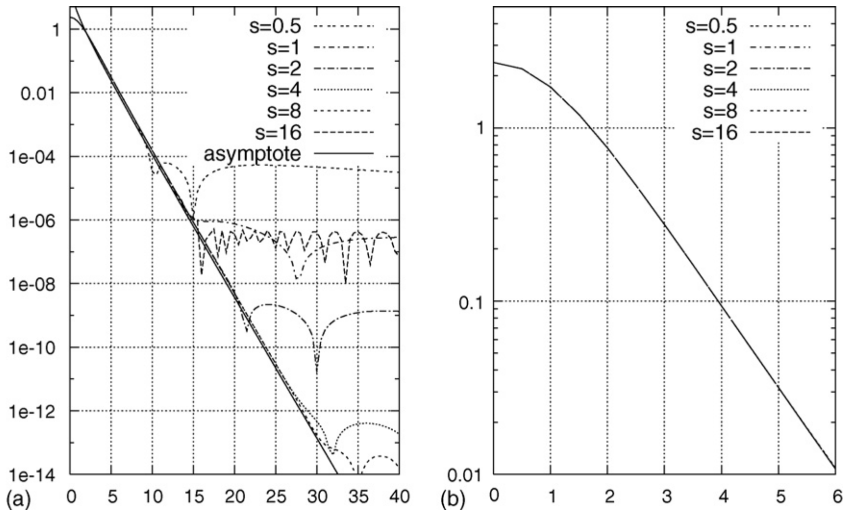

Fig. 2. Profile of solution $u(r)$ as obtained with different scales and the same number of functions $N = 50$: (a) asymptotic behavior and (b) energy containing range.

Note the cusps formed by some of the lines. They correspond to the number for which the actual coefficients become negative. The effectiveness of the method in this case is really impressive. Taking just 50 functions allows one to obtain the solution with accuracy 10^{-5}.

Another important characteristic of the method is the extent to which the first several coefficients are affected by the total number N of functions taken. Fig. 1(b) shows that the first 20 coefficients are indistinguishable for $N = 40$, 90, and 200. What is even more amazing is that an accuracy of 10^{-4} is obtained with just 20 functions. We shall call these first 20 members of the Galerkin series "the energy containing modes". Respectively, the domain where the profile is larger than 10^{-2} will be called "energy containing range".

The next verification is to examine the asymptotic behavior of the solution in the configurational space. As shown above, the asymptotic behavior of the functions of our system is x^{-1} for the odd sequence, and x^{-2} for the even. At the same time the solution with radial symmetry that decays at infinity has the following asymptotic behavior:

$$u(r) \sim K_0(r) \sim r^{-(1/2)}\,\mathrm{e}^{-r}, \quad r \to \infty,$$

where the modified Bessel function of the second kind, $K_0(r)$, is the solution of the linearized Boussinesq equation with the proper behavior at infinity. We solved the problem numerically with several different values for the scale $\lambda^{-1} = \mu^{-1} = s$ and $N = 50$. Fig. 2(a) shows the asymptotic behavior of the profile of the axisymmetric solution for different values of the scale. It is clear that there exists an optimal scale $s \in [4, 8]$ for this particular problem because the asymptotic behavior is unsatisfactory for both $s < 4$ and $s > 8$.

6. Results and discussion

As mentioned in the previous section, when $c_1 = c_2 = 0$, the solution is axisymmetric. Then the soliton has perfect bell shape and the (contour) lines of equal height are concentric circles.

Our numerical investigation unearthed a very peculiar property of the problem under consideration, namely that the solution shape is not structurally stable when small deviations from radial symmetry are introduced. The meaning is that even for small deviations of c_1, c_2 from zero, an important property such as the asymptotic law of decay changes radically, Our results confirm similar findings obtained with the finite-difference method of [8]. In order to investigate this symmetry breaking we did calculations with $c = 0$ and several small values for c_2. Fig. 3 shows the result in logarithmic scale that allows one to discern the tails of the solutions better. For comparison, we note that for $c = 0$, Fig. 2(a) shows that the decay is asymptotic down to 10^{-12} which is the limit of calculations with double precision. It is clearly seen in Fig. 3 that even for very small $c = 0.005$ the asymptotic behavior of the solution departs from

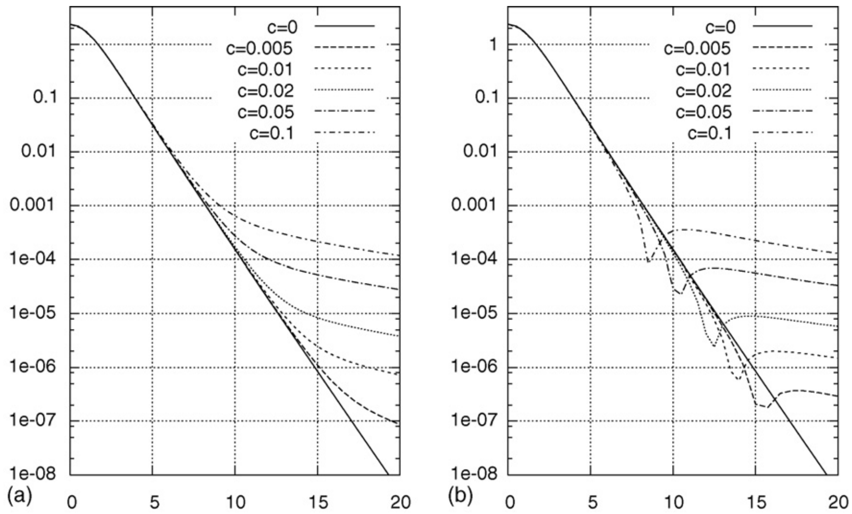

Fig. 3. Evolution of the solution with c_2 for $c_1 = 0$ in the two main cross-sections of the 2D shape: (a) $y = 0$ and (b) $x = 0$.

the exponential decay at 10^{-7} which is five orders of magnitude larger. Hence one can conclude that the change of asymptotic behavior is not a round-off effect.

For $|c| \neq 0$, the actual asymptotic behavior at infinity is as x^{-2} and y^{-2}, for the $y = 0$ and $x = 0$ cross-sections, respectively. Since the asymptotic behavior of the functions of our CON system is also second order, one can suspect that the observed asymptotic behavior is an artifact of the expansion. Yet, for $c = 0$ the same system of functions gave perfect exponential decay down to the round off error, with as few as 50 members of the series. In order to clarify this issue, we compare our solution for $c = 0$, $c_2 = 0.6$ with the difference solution of [8]. This is demonstrated in Fig. 4 for $c_1 = 0$ and $c_3 = 0.6$.

In Fig. 5, we present the soliton solution when the phase speed along the x-axis is $c_1 = 0$ while the phase speed along the y-axis is $c_2 = 0.7$ which is fairly large value, close to the critical phase speed $c_2 = 1$. The interesting observation here is that the soliton develops negative forerunner and back runner (depressions). At the same time, the main hump is relatively contracted in the direction of motion (the y-axis) while the overall support of the soliton is enlarged proportionally to the pseudo-Lorentzian factor $\sqrt{1 - c_2^2}$.

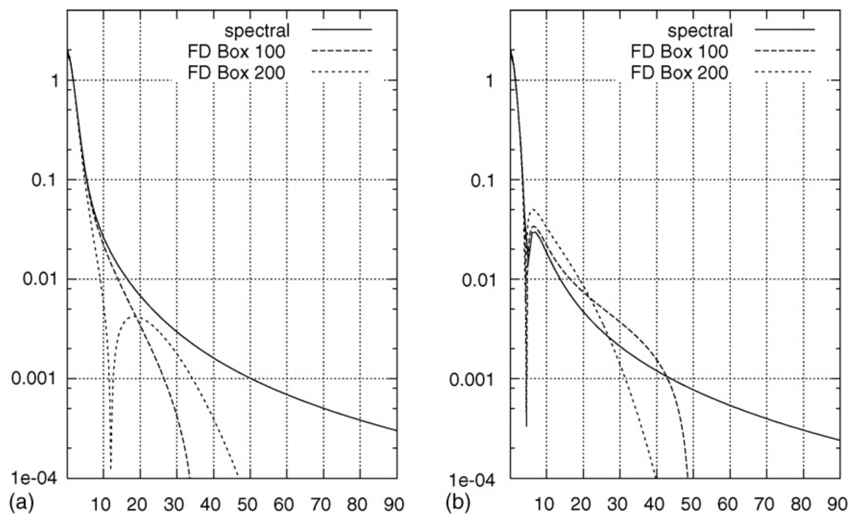

Fig. 4. Comparison with the FD solution of [8] in asymptotic range for the two main cross-sections: (a) $y = 0$ and (b) $x = 0$.

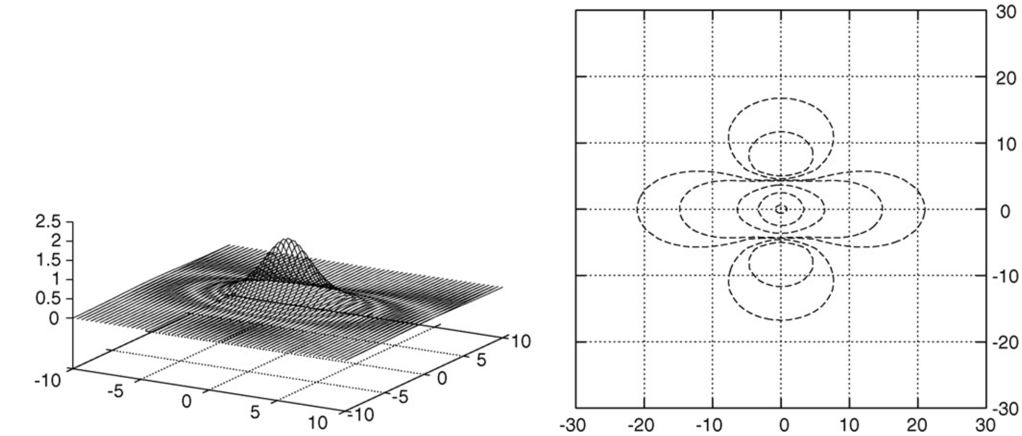

Fig. 5. Left: soliton shape for $c_1 = 0$, $c_2 = 0.7$, $\lambda = \mu = 4$ and $N = 20$. Right: contour lines 1.2, 0.4, 0.1, 0.02, 0.01, −0.01 and −0.02.

This effect is clearly seen in the right panel of Fig. 5 where the contour lines for several typical values are presented. The negative contour values are not commensurate with the spacing of contours in the positive part of the solution, because the depressions ahead and behind the propagating solitary wave are very shallow in comparison with the height of the main hump. One sees that the cross-sections are no longer circles, but ovals whose short axes are aligned with the direction of motion.

To confirm the hypothesis that the short axes of the ovals are aligned with the direction of motion we did different computations with different components of the phase velocity, while keeping the modulus the same. We chose an extremely large phase speed $|c| = 0.9$ which presents a tough computational case because of the enlarged support of the wave. The results for the different orientations of the velocity vector of the center of soliton are presented in the series of figures (Fig. 6). The first figure is for $c_1 = 0$ and $c_2 = 0.9$ (the soliton moves along the y-axis), the second

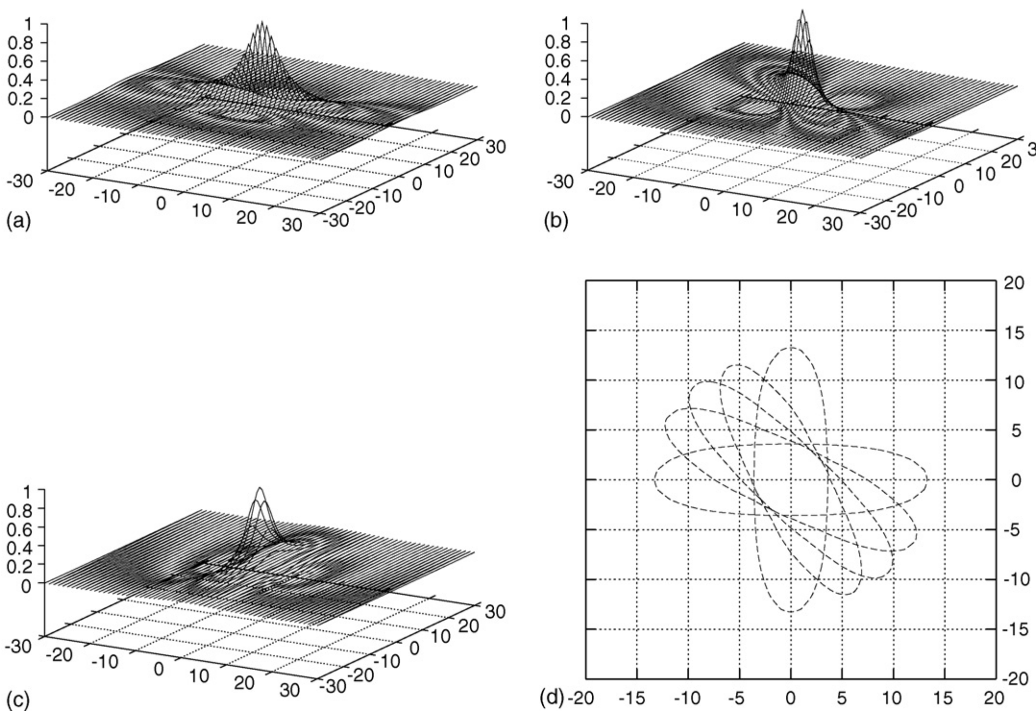

Fig. 6. (a–c) Soliton shape for $c_1^2 + c_2^2 = c^2 = 0.9$ but different c_1, c_2, $\lambda = \mu = 4$ and $N = 20$. (d) The contour line 0.1 for five different solitons with $c = 0.9$.

is for $c_1 = c_2 = \sqrt{0.405} \approx 0.6364$ (the soliton moves along the bisector of first quadrant), and the third figure is the case $c_1 = 0.9$ and $c_2 = 0$ (soliton moves along the x-axis). Together with its physical importance, the good agreement between different shapes (after rotated on 45° or 90°), presents additional verification of the algorithm, because of the different spectral composition of solution. For the two limiting cases, when the soliton moves along one of the axes, the series contain only the even sequence of functions, while the other cases involve also the subsequence of odd functions.

Fig. 6(d) presented the contour line 0.1 for different components of the phase speed. It is clearly seen that the short axis of the oval is aligned with the direction of motion. If rotated, the ovals are virtually indistinguishable, which is an important verification of the method.

7. Conclusions

In the present paper, the Fourier–Galerkin spectral technique used in previous authors' works in 1D, is applied to computing the stationary propagating localized solutions of the 2D Boussinesq equation. The basis is a complete orthonormal sequence in $L^2(-\infty, \infty)$ for which the products of nonlinear terms can be expressed into series with respect to the system. For the fine tuning of the algorithm, scaling factors, λ and μ are introduced for the independent variable. The algorithm is thoroughly validated by means of self-consistency tests involving different number of functions and different values for the scaling parameters. The exponential convergence of the Fourier coefficients is confirmed by the calculations. Results are compared with existing difference solutions and is shown that they are in good agreement.

The technique developed is used to obtain the shapes of the solitary waves for different phase velocities. The shape of the axisymmetric wave at rest resembles very much the shape of the 1D *sech*-soliton of Boussinesq equation, with the only difference that the 2D shape is higher. Similarly to the 1D case, the support of the propagating waves is increased by the inverse of the Lorentz factor. An important physical finding in 2D is, that while the overall length of the support increases, the dimension in the direction of motion is contracted relative to the transverse direction. In this sense, an overall expansion of the shape is observed with relative contraction in the longitudinal direction, i.e. the shapes appear to spread more for larger phase speeds, but are relatively "squashed" in the direction of motion. This is in agreement with our earlier finite-differences computations.

The results obtained here are encouraging and open the possibility of applying the Fourier–Galerkin method to 2D time dependent problems which will allow investigation of the interaction of solitons in the cases when no analytical solutions are available.

References

[1] M.J. Ablowitz, H. Sigur, Solitons and the Inverse Scattering Transform, SIAM, Philadelphia, 1981.
[2] J.V. Boussinesq, Théorie des ondes et des remous qui se propagent le long d'un canal rectangulaire horizontal, en communiquant au liquide contenu dans ce canal des vitesses sensiblement pareilles de la surface au fond, Journal de Mathématiques Pures et Appliquées 17 (1872) 55–108.
[3] J.P. Boyd, The asymptotic coefficients of Hermite series, J. Comp. Phys. 54 (1984) 382–410.
[4] J.P. Boyd, Spectral methods using rational basis functions on an infinite interval, J. Comp. Phys. 69 (1987) 112–142.
[5] J.P. Boyd, The orthogonal rational functions of Higgins and Christov and algebraically mapped Chebishev polynomials, J. Approx. Theory 61 (1990) 98–105.
[6] J.P. Boyd, Chebyshev and Fourier Spectral Methods, Dover Press, 2000.
[7] R.K. Bullough, F. Caudrey, Soliton and its history, in: R.K. Bullough, F. Caudrey (Eds.), Solitons, Springer, Berlin, 1980, pp. 11–77.
[8] J. Choudhury, C.I. Christov, 2D solitary waves of boussinesq equation, in: A. Ludu, N. Hutchings, D. Fry (Eds.), ISIS International Symposium on Interdisciplinary Science, Natchitoches, Washington, DC, October 6–8, 2004, AIP Conf. Proc. 755 (2005) 85–90.
[9] M. Christou, C.I. Christov, Fourier–Galerkin method for localized solutions of the sixth-order generalized boussinesq equation, in: J. Du, S. Hu (Eds.), Proceedings of the International Conference on Dynamical Systems & Differential Equations, Atlanta, 2000, Added Volume to "Discrete and Continuous Dynamical Systems", 2001, pp. 121–130.
[10] M. Christou, C.I. Christov, Fourier–Galerkin method for localized solutions of equations with cubic nonlinearity, J. Comput. Anal. Appl. 4 (1) (2002) 63–77.
[11] M.A. Christou, C.I. Christov, Fourier–Galerkin method for interacting localized waves, J. Neural Parallel Sci. Comput. 4 (1) (2002) 63–77.
[12] M.A. Christou, C.I. Christov, Localized waves for the regularized long wave equation via a Galerkin spectral method, J. Math. Comp. Simul. 69 (2005) 257–268.
[13] C.I. Christov, A complete orthonormal sequence of functions in $L^2(-\infty, \infty)$ space, SIAM J. Appl. Math. 42 (1982) 1337–1344.

[14] C.I. Christov, Fourier–Galerkin algorithm for 2D localized solutions, Annuaire de l'Univ. Sofia, Livre 2-Mathématiques Appliqee et Informatique 89 (1995) 169–179.
[15] C.I. Christov, K.L. Bekyarov, A Fourier-series method for solving soliton problems, SIAM J. Sci. Stat. Comp. 11 (1990) 631–647.
[16] J.R. Higgins, Completeness and Basis Properties of Sets of Special Functions, Cambridge University Press, London, 1977.
[17] D.J. Korteweg, G. de Vries, On the change of form of long waves advancing in a rectangular canal, and on a new type of long stationary waves, Philos. Magn. 39 (1895) 422–443 Ser. 5.
[18] A.C. Newell, Solitons in Mathematics and Physics, SIAM, Philadelphia, 1985.
[19] N. Wiener, Extrapolation, Interpolation and Smoothing of Stationary Time Series, Technology Press MIT/John Wiley, New York, 1949.
[20] N.N. Yanenko, Method of Fractional Steps, Gordon and Breach, 1971.